The EMBO Journal vol.7 no.11 pp.3397-3405, 1988

Evidence for a nuclear factor(s), IRF-1, mediating induction and silencing properties to human IFN-β gene regulatory elements

Takashi Fujita, Jun Sakakibara, Yoshiaki Sudo[1], Masaaki Miyamoto, Yoko Kimura and Tadatsugu Taniguchi

Institute for Molecular and Cellular Biology, Osaka University, Suita-shi, Osaka 565, Japan

[1]Present address: Research Laboratories, Sumitomo Pharmaceutical Co. Ltd, Kasugade, Konohanaku, Osaka 554, Japan

Communicated by P.Rigby

Transcription of the human interferon-β (IFN-β) gene is induced by a variety of agents such as viruses, dsRNA and some cytokines. In this study, we describe a nuclear factor, termed interferon regulatory factor-1 (IRF-1), that is involved in the transcription of IFN-β and possibly other genes. We demonstrate that IRF-1 functions in virus-induced transcription by interacting with previously identified, IFN-β regulatory DNA elements. Our data suggest that IRF-1 participates in the transient formation of an induction-specific complex(es) with the regulatory elements. IRF-1 may also be involved in silencing the function of the SV40 enhancer juxtaposed to the regulatory elements in uninduced cells.

Key words: interferon/regulatory factor/cytokine/regulatory DNA

Introduction

Interferons (IFNs) belong to a family of cytokines and deliver various signals to target cells. Like most of the cytokines, expression of their genes is primarily controlled at the transcriptional level. In the case of type I IFNs, transcription of both IFN-α and IFN-β genes is transiently induced by a variety of agents such as viruses and dsRNA. A number of expression studies with cloned IFN-α and IFN-β genes have revealed the presence of *cis*-acting DNA sequences that mediate the virus-induced activation of transcription within the 5'-flanking region (for reviews see Stewart, 1979; Lengyel, 1982; Weissmann and Weber, 1986; Taniguchi, 1988).

In the human IFN-β gene, repetitive hexanucleotide units are present quasi-tandemly within the region spanning between −65 and −109 relative to the cap site (Fujita *et al.*, 1985). Previously, we, as well as others, have shown that this region is responsible for the induced transcriptional activation of IFN-β gene (Ohno and Taniguchi, 1983; Zinn *et al.*, 1983; Dinter *et al.*, 1983; Fujita *et al.*, 1985). In addition, we have presented evidence for an incremental role of such core unit sequences in induction; each of the units constitutes an inducible element which co-operates for the maximal induction of the gene (Fujita *et al.*, 1987). Interestingly, such sequence motifs are also found in other virus-inducible cytokine genes such as IFN-α_I1, IFN-α_{II}1, tumor necrosis factor-α (TNF-α) and interleukin-6 (IL-6) (Fujita *et al.*, 1987; Yasukawa *et al.*, 1987). Our *in vivo* DNA competition assays provided evidence that a positive regulatory factor(s) interacts with such elements. More recently, it was shown that such elements manifest a reversible silencing property to the function of the closely linked SV40 or CMV enhancers (Kuhl *et al.*, 1987; mentioned in Fujita *et al.*, 1987). In the present study, we describe the identification and characterization of a nuclear factor, designated as interferon regulatory factor-1 (IRF-1), that specifically binds to IFN-β gene inducible elements. We provide evidence that the factor plays an essential role in the viral induction of IFN-β gene transcription. We also provide evidence for the involvement of IRF-1 in the previously described silencing of SV40 enhancer by the adjoined inducible elements in uninduced cells.

Results

Identification of nuclear factors binding to upstream sequences of IFN-β gene

We first attempted to identify nuclear factors in mouse L929 cells which specifically bind to the 5' upstream sequence of human IFN-β gene by a gel shift assay (Singh *et al.*, 1986). This cell line was chosen, since most of our previous gene transfer studies on the IFN-β gene regulation have been carried out using this cell line as the recipient (Fujita *et al.*, 1985, 1987). In this assay, we used a 219 bp DNA segment containing the IFN-β gene sequence spanning between −105 and +19 (relative to the cap site), containing the regulatory elements (Figure 1A).

Crude nuclear extracts were prepared from Newcastle disease virus (NDV)-induced mouse L929 cells. Since, specific complexes were hardly detectable with the crude extracts (data not shown), we fractionated the extracts by Heparin Sepharose column chromatography. Most of the specific DNA-binding activity was recovered within the fractions eluted with 0.2 and 0.3 M KCl (data not shown). At least three shifted bands could be identified in this assay and they were termed complex 1, 2 and 3 (Figure 1B). In this analysis, the shift pattern was essentially the same with extracts from induced and mock-induced cells, but the intensity of the shifted bands was significantly stronger (2- to 3-fold) with extracts from induced cells (data not shown; see below). Treatment of the binding mixture with proteinase K abolished the appearance of the shifted bands, indicating that the complexes are essentially formed by the probe DNA and protein factor(s) (data not shown).

To assess the binding specificity, we next performed a series of DNA competition assays. When unlabeled probe DNA, or IFN-β gene DNA fragments derived either from deletion mutants pBR-93 or pBR-80 were added in molar excess over the labeled probe to the binding mixture, formation of all three complexes was inhibited to a significant degree (Figure 1B, lanes 3−7). In contrast, the DNA fragment containing sequence −66 to +19 failed to inhibit

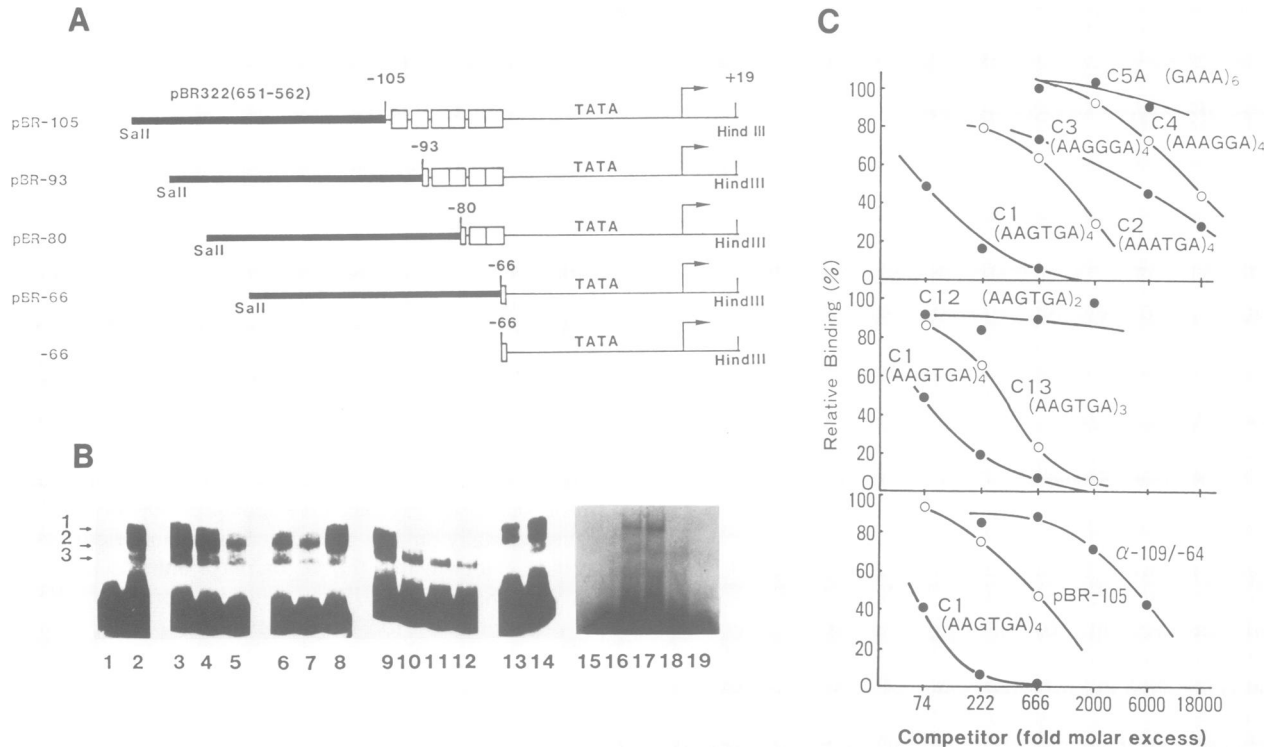

Fig. 1. Detection of nuclear factors which bind to 5′ upstream sequences of the human IFN-β gene. (**A**) DNA fragments used as probes and competitors. Open boxes each represent a hexamer repeat unit within the human IFN-β gene (Fujita *et al.*, 1985). Arrows indicate the transcription initiation site. The thick line indicates DNA sequence derived from pBR322 (651−562). (**B**) Gel shift assay. End-labeled pBR-105 (lanes 1−14) or pBR-66 (lanes 15−19) were used as probe (1 fmol). The reaction mixture consisted of (Materials and methods) no nuclear extract (lanes 1 and 15) or contained Heparin Sepharose fractionated extract from induced L929 cells (1 μg) (lanes 2−14, 16−18) or nuclear factor purified by DNA affinity chromatography from induced L929 cell (3 μg) (lane 19) (see Materials and methods for details). In the competition assay, the following unlabeled DNA was added in molar excess over the probe DNA in the reaction mixture: lanes 3, 4, 5: pBR-105 DNA in 79, 238 and 714 fmol, respectively; lane 6: pBR-93 DNA, 714 fmol; lane 7: pBR-80 DNA, 714 fmol; lane 8: pBR-66 DNA 714 fmol; lanes 9−12: C1 oligomer, 74, 222, 666 and 2000 fmol, respectively; lane 13: SV40 enhancer (200 bp *Xho*I fragment, Banerji *et al.*, 1981) 1360 fmol; lane 17: C1 oligomer, 1 pmol; lane 18: SV40 enhancer (above), 1 pmol. (**C**) Inhibition of complex 1 and 2 formation by functional or non-functional DNA segments in conferring virus-inducibility. Gel shift assay was performed by using the labeled pBR-105 as probe and various unlabeled DNA fragments as competitors. The formation level of complex 1 and 2 was quantitated by densitometric analysis of the autoradiogram. Complex formation in the absence of unlabeled competitor DNA was taken as 100%. **Upper panel**: competition by repeated oligomers with various hexamer unit sequences. **Middle panel:** competition by oligomers with various repeats of the AAGTGA sequence. **Lower panel:** competition by the DNA segments containing IFN-α1 and IFN-β regulatory elements.

the formation of complexes 1 and 2 but did inhibit complex 3 (lane 8). Nuclear factor(s) giving rise to complex 3 might be involved in the expression of a variety of other genes, in view of the finding that the appearance of this band is inhibited by the SV40 enhancer sequences (lanes 13 and 18).

Correlation between the factor-binding affinity of the various oligomers and their virus-inducibility

We have previously shown that repeated synthetic hexamers function as virus-inducible *cis*-acting elements when placed upstream of cognate or non-cognate promoters (Fujita *et al.*, 1987). Among the various hexamer sequences tested, transcriptional activation in the NDV-induced L929 cells was observed with 4-fold-repeated hexamers in the following order of efficiency; $(AAGTGA)_4$, $(AAATGA)_4$, $(AAGGGA)_4$, $(AAAGGA)_4$. We also obtained evidence by *in vivo* competition experiments that native IFN-β upstream sequence and hexamer repeat $(AAGTGA)_8$ can bind to a common positive regulatory factor(s) (Fujita *et al.*, 1987). As shown in Figure 1(B), specific inhibition of complex (1 and 2) formation was also observed by the hexamer repeat $(AAGTGA)_4$ (lanes 10−12).

In view of those findings, we next examined whether the efficiency of inducibility of those oligomers (designated as C1, C2, C3, C4 and C5A, in Figure 1C) correlates with their affinity to the putative factor(s) involved in complex formation. Actually, unlabeled oligomers were added at different concentrations in the binding mixture described in the previous section and the relative intensity of the shifted bands was monitored. As summarized in Figure 1(C), synthetic oligomers C1, C2, C3 and C4 specifically competed in the formation of complexes 1 and 2, indicating that a common factor(s) is binding to native and synthetic sequences. The binding affinity of the oligomer in this assay was in the respective order of C1, C2, C3, C4 and very low with C5A (Figure 1C). Thus, the binding affinity of each of the oligomers to the factor(s) is in correlation with its efficiency to virus-inducibility. We had previously shown that the decrease in the number of (AAGTGA) repeat units from four to three reduced the inducibility by a factor of 10. The inducibility was below detectable levels when the number of repeats was reduced to two (Fujita *et al.*, 1987). Again, a significant correlation was seen between the factor-binding affinity and virus inducibility in those oligomers (Figure 1C). Formation of both complex 1 and 2 is also inhibited by a 46 bp DNA segment (VRE) derived from the human IFN-α1 promoter (Ryals *et al.*, 1985), albeit with much lower efficiency. Taken together, a common protein

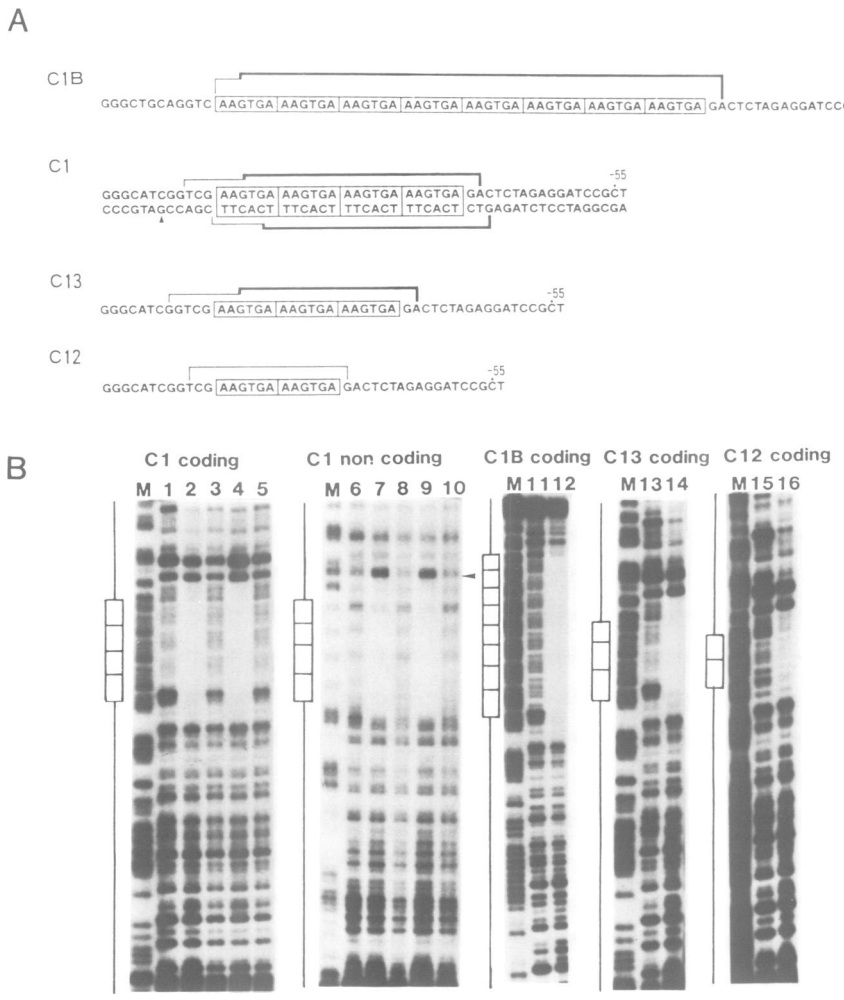

Fig. 2. Binding of IRF-1 to hexamer (AAGTGA) repeats. (**A**) Region of the nucleotide sequence of probes used for footprint analysis. Only the strands which were subjected to analysis are indicated. Strongly or weakly protected nucleotides are indicated by surrounding thick and thin lines, respectively. Arrowhead: DNase I hypersensitive nucleotide due to factor binding. (**B**) Binding of IRF-1 to the hexamer repeat sequences. The following DNA segments were used for analysis: C1B, *SalI*−*Hin*dIII fragment of p-55C1B; C1, C13 and C12, *AvaI*−*Hin*dIII fragment of p-55C1, p-55C13 and p-55C12, respectively (Fujita *et al.*, 1987). Probes labeled either in the coding strand (lanes 1−5, 11−16) or in the non-coding strand (lanes 6−10) were used. The position of the (AAGTGA) unit sequence is indicated as boxes in the left side of each panel. Reaction mixture was assembled as described in Materials and methods. M: End-labeled probe DNA, subjected to the A+G chemical sequencing reaction (Maxam and Gilbert, 1980); lanes 1, 6, 11, 13, 15: no nuclear extract; lanes 4, 5, 9, 10, 12, 14, 16: 1 μg of Heparin Sepharose fractionated extract from induced L929 cell; lanes 2, 3, 7, 8: 1 μg of Heparin Sepharose fractionated extract from mock-induced L929 cell; lanes 3, 5, 8, 10: 1000-fold molar excess of cold C1 oligomer was added to the reaction mixture; arrowhead: position of the hypersensitive nucleotide.

factor seems to be involved in the formation of complexes 1 and 2 (also, see below). We tentatively designate the factor as interferon regulatory factor-1 (IRF-1).

Footprint analysis of IRF-1 bound to the hexamer (C1) repeats

To examine the nature of IRF-1 binding to the virus-inducible elements, we performed a DNase I footprint analysis (Lefevre *et al.*, 1987). Nuclear extracts were prepared either from NDV-induced or mock-induced L929 cells and fractionated as described above and the DNA probes each containing different numbers of the C1 hexamer sequence were used for the analysis (Figure 2A). Three, four or eight tandemly repeated hexamers (AAGTGA) endowed complete protection. However, a relatively weak protection was observed with the dimeric hexamer (Figure 2B). Thus, the affinity of IRF-1 to the dimer is considerably lower than the others, indicating a certain co-operativity of IRF-1 binding to the regulatory elements (see also Figure 1C). Such a co-operativity might be important in gene induction since the dimeric hexamer is unable to confer detectable inducibility to the truncated IFN-β promoter in L929 cells (Fujita *et al.*, 1987).

In the coding strands of C1 and C13 probes, all the hexamer units and the additional four and two nucleotides upstream and downstream of the units, respectively, were protected. However, with C1B which has different flanking sequences compared to other gene constructs (see Figure 2A), no additional nucleotides in the upstream region were protected. The weak protection of the additional nucleotides might be due to permutations in the hexamer units (see Figure 2A); i.e. the actual recognition sequence of IRF-1 in the coding strand of those probes may be GTGAAA and IRF-1 weakly recognizes the GTCGAA sequence present in the protected upstream region of C1 and C13 but not C1B. For the non-coding strand, protection can be seen nearly in a symmetrical manner to the coding strand as far as the C1 probe is concerned (Figure 2B). Essentially the same results

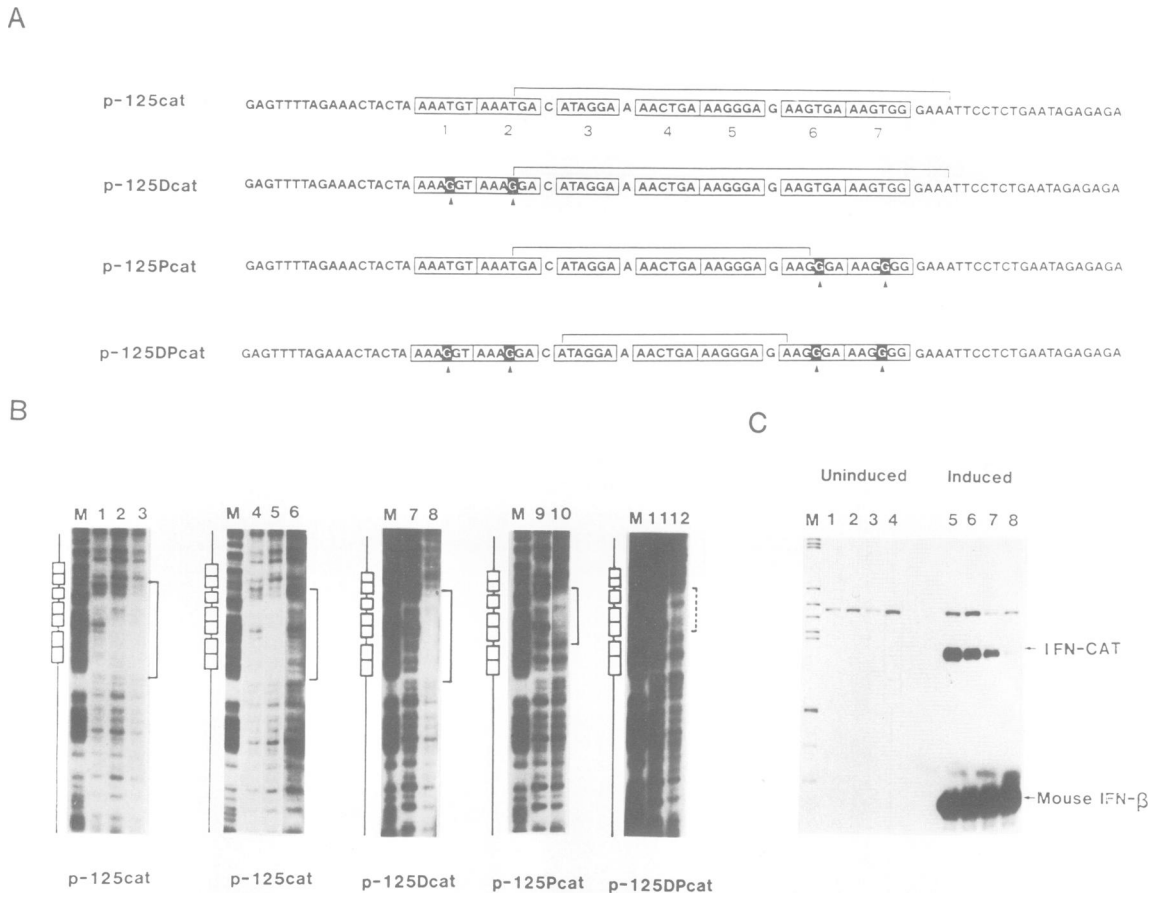

Fig. 3. Effect of point mutations on IRF-1 binding and their virus-inducibility. (**A**) Part of the nucleotide sequence of wild-type (p-125cat) and point mutants. The homologous hexamer sequence present in human IFN-β gene (Fujita *et al.*, 1985) is framed (1–7). Positions of introduced transversions are indicated by arrowheads. Lines indicate DNase I protected region by 3 μg of partially purified IRF-1. (**B**) Binding of IRF-1 to wild type or mutant IFN-β regulatory elements. *Hin*dIII–*Sal*I fragment labeled at the *Hin*dIII end in the non-coding strand from p-125cat (lanes 1–6), p-125Dcat (lanes 7, 8), p-125Pcat (lanes 9, 10) and p-125DPcat (lanes 11, 12) were used as probes. M: chemically cleaved probe DNA (A+G reaction), lanes 1, 4, 7, 9, 11: no extract; lane 2: 1.5 μg of the DNA affinity purified IRF-1 from induced L929 cells (see Materials and methods); lanes 3, 5, 6, 8, 10, 12: 3 μg of IRF-1; lane 6: as lane 5 except 1000-fold molar excess of unlabeled C1 oligomer added to the reaction mixture; boxes in each panel represent the homologous hexamer units. (**C**) Effect of point mutations in the hexamer units on virus inducibility. Stable L929 cell transformants carrying p-125cat (lanes 1, 5), p-125Dcat (lanes 2, 6), p-125Pcat (lanes 3, 7), p-125DPcat (lanes 4, 8) were mock-induced (lanes 1–4) or induced by NDV (lanes 5–8) for 10 h. Correctly initiated transcripts from introduced IFN–CAT genes and endogenous mouse IFN-β gene (arrows) were quantitated by S1 analysis. M: size markers (end-labeled *Hae*III fragments of pBR322). The largest fragment shown in this figure is 504 nt long.

were obtained by using the nuclear extract from uninduced cells. No significant protection of the IFN-β promoter region (−55 to +19) by a factor(s) giving rise to complex 3 could be detected by this analysis.

Nature of IRF-1 binding to wild-type and mutant IFN-β regulatory elements

To investigate the nature of the IRF-1 binding to the IFN-β gene regulatory elements, we performed DNase I footprint analysis with IRF-1 partially purified by the DNA affinity column chromatography (see Materials and methods). The IFN-β sequence (−125 to +19) was terminally labeled at position +19 and used as the probe. When 1.5 μg of the partially purified IRF-1 was included in the reaction mixture, nucleotides between −80 and −70 were protected with the wild-type gene (Figure 3B). Notably, the protection was extended further (−100 to −61) by doubling the amount of IRF-1 in this analysis (Figure 3B). The results suggest that blocks 6 and 7 have higher affinity to IRF-1 when compared to other upstream blocks. The results may explain the observation made in Figure 1(B), in which 714-fold molar excess of the DNA segment derived from pBR-80 (containing blocks 6 and 7) competed with IRF-1 binding as efficiently as that derived from pBR-105 (containing four additional blocks) in those assays. Thus, one might expect to detect a difference when the ratio of probe to competitor DNA is altered. As expected, the addition of molar excess C1 oligomer abolished the footprinting completely (Figure 3B). The similarly purified IRF-1 from the mock-induced cells showed identical results (data not shown).

Previously, we had provided evidence that the presence of pyrimidine residues in hexamer repeats greatly contribute in the induction efficiency of the repeats. In fact, a change in the hexamer unit sequence (AAGTGA) to (AAGGGA) and in (AAATGA) to (AAAGGA) reduced the induction levels 6- and >15-fold, respectively (Fujita *et al.*, 1987). Based on this finding, we introduced T to G transversions in some of the T residues within the hexanucleotide units of the natural IFN-β sequence expecting that such a mutation may result in the reduction of both IRF-1 binding affinity and induction levels (Figure 3A). We linked the bacterial chloramphenicol acetyltransferase (CAT) reporter gene

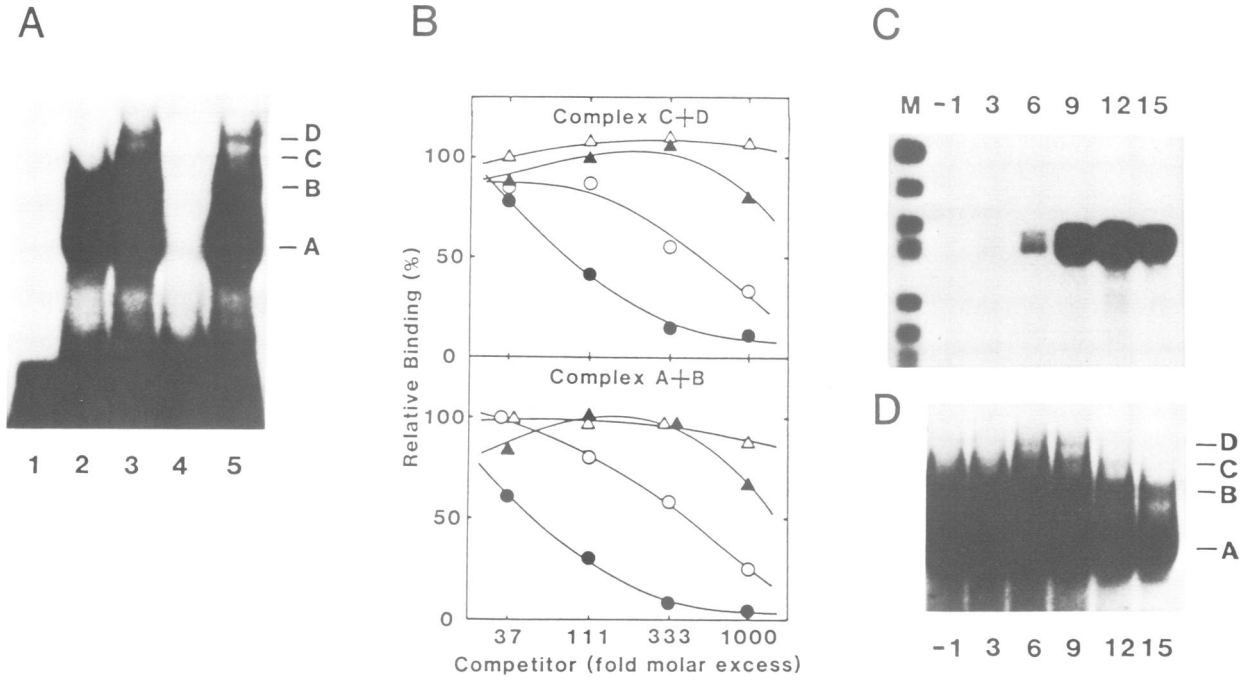

Fig. 4. Detection of the induction-specific complexes. (**A**) Gel shift analysis of mock-induced and NDV-induced whole cell extract. End-labeled C1 oligomer was used as the probe. Lane 1: no extract; lane 2: 3 μg of mock-induced L929 whole cell extract; lanes 3–5: 3 μg of whole cell extract from 8-h induced L929 cells; lane 4: as lane 3 except 2000-fold molar excess of cold C1 oligomer was added to the reaction mxiture; lane 5: as lane 3 except 2000-fold molar excess of cold C5A oligomer was added to the reaction mixture. Positions of complexes (A, B, C and D) are indicated. (**B**) DNA competition assays for testing the affinity of the four protein–DNA complexes observed in (A). The assays were carried out essentially as described in Figure 1C. Competitor DNAs are: C1 (●), C2 (○), C3 (▲) and C4 (△). Levels of the complexes A+B and C+D were measured by densitometric scanning of the autoradiogram. For complexes A+B, the film was exposed for 12 h and for complexes C+D, 24 h. (**C**) Time course of endogenous mouse IFN-β mRNA accumulation. At indicated times after NDV infection, L929 cells were harvested and cytoplasmic mouse IFN-β mRNA was quantitated by S1 analysis. M: size markers as Figure 3C. (**D**) Time course of the appearance of the induction-specific complexes. Part of the cells harvested for the mRNA accumulation was taken to prepare the whole cell extract and subjected to gel shift analysis as in Figure 3C.

downstream of the respective wild-type and mutant IFN-β gene sequences in order to monitor the induction level (see Figure 3A).

The mutation in blocks 6 and 7 (p-125Pcat) resulted in a dramatic reduction of IRF-1 binding to those blocks, whereas other blocks (3, 4 and 5) still remained protected by IRF-1 (Figure 3B). The induction level of the mutant gene, stably introduced into the chromosomes of L929 cells was 6-fold lower than that of the wild-type gene (Figure 3C). Mutation of elements 1 and 2 (p-125Dcat) did not result in a significant change in the footprint pattern from that of the wild-type gene (Figure 3B), but a significant reduction (50%) in induction level was observed (Figure 3C). Moreover, the mutant gene (p-125DPcat) with point mutations within the four blocks (1, 2, 6 and 7) showed only a weak protection of blocks 3, 4 and 5 by IRF-1 in this assay. Reduction of inducibility with this mutant gene was 20-fold compared to the wild-type (Figure 3C), again suggesting the contribution of blocks 1 and 2 in the induction. The inducibility of various mutant genes was also tested by the transient expression system leading to similar conclusions (data not shown).

Detection of the induction-specific factor–DNA complexes

The data presented above suggest that IRF-1 plays a role in the NDV-induced IFN-β gene expression in L929 cells. However, the extraction and purification methods of IRF-1 applied did not permit us to gain insights on the induction specific events occurring in IRF-1. Possibly, only a limited number of the IRF-1 goes through modifications to convert into active form or the active form is very unstable, or both. We therefore employed a different method for the preparation of the cell extracts (see Materials and methods for the details) and subjected the extract to gel shift assay by using the C1 oligomer as the probe DNA. In addition to complexes A and B, which can be found in the extracts from both induced and mock-induced cells, two additional complexes (C and D) became detectable by using the extract from NDV-induced but not from mock-induced cells (Figure 4A). The complex formation is also inhibited by C1 but not by C5A oligomers. Furthermore, when we tested the affinities of the protein involved in the specific complex formation to various oligomers by using the same approach described above (Figure 1C), they were indistinguishable from those of IRF-1 (Figure 4B). The appearance of this induction-specific complex(es) is transient and it correlates well with the appearance of induced IFN-β mRNA (Figure 4C).

Silencing effect of the inducible elements and IRF-1 binding

Using the transient expression system, we previously observed that the hexamer repeat $(AAGTGA)_8$ interposed between the SV40 enhancer and a truncated (−55) IFN-β promoter, almost completely suppressed (or silenced) the function of the enhancer unless the cells were virally induced

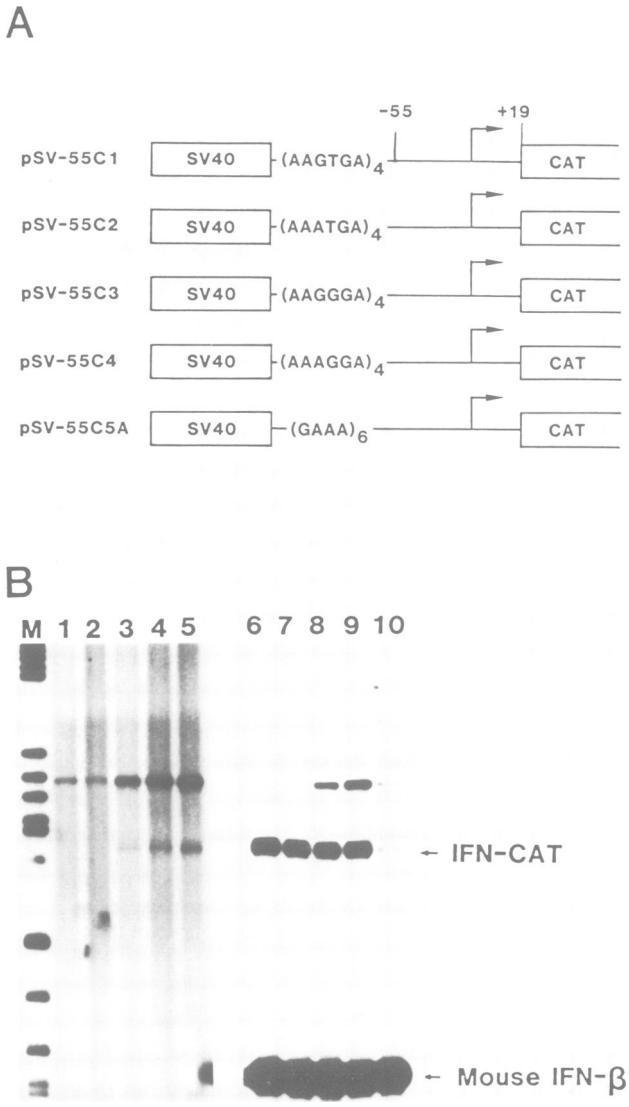

Fig. 5. Reversible silencing effect of various synthetic oligomer sequences. (**A**) Structure of the test genes. Various hexamer or tetramer repeats were each interposed between SV40 enhancer (SV40) and IFN-β silent promoter (-55 to $+19$) (Fujita *et al.*, 1987; Maruyama *et al.*, 1987). Arrows indicate the transcription initiation site. (**B**) S1 analysis. Stable L929 cell transformants carrying pSV-55C1 (lane 1, 6), pSV-55C2 (lanes 2, 7), pSV-55C3 (lanes 3, 8), pSV55C4 (lanes 4, 9) and pSV-55C5A (lanes 5, 10) were mock-induced (lanes 1–5) or induced by NDV for 10 h (Materials and methods). Transcripts were quantitated by S1 analysis as Figure 3C. Autoradiography was carried out by exposing the films for 72 h (lanes 1–5) and for 20 h (lanes 6–10).

(in Fujita *et al.*, 1987). More extensive studies on this silencing effect have been carried out by Kuhl *et al.* (1987). They found that the tetrameric hexamers (GAAAGT) and (AAGTGA) but not a pBR322-derived DNA with the same length specifically silenced the function of SV40 enhancer when interposed between the enhancer and rabbit β-globin promoter in uninduced L929 cells. To gain insight on this phenomenon, we examined the silencing effect of various hexamer repeats, whose inducibility and affinity to IRF-1 had been characterized.

Chimeric genes were constructed as depicted in Figure 5A and introduced into L929 cell chromosome by co-transformation (see Materials and methods). The S1 mapping analysis revealed that, in uninduced cells, expression of the

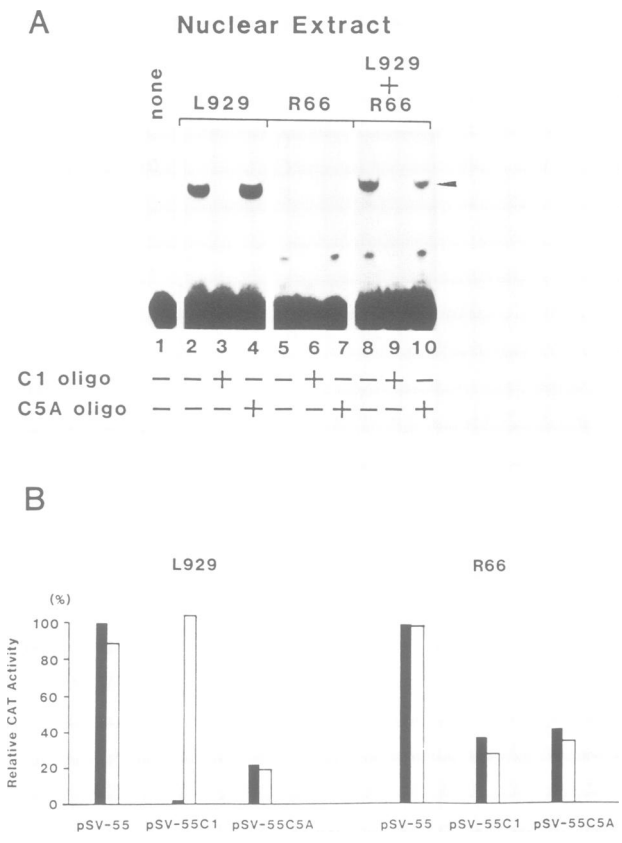

Fig. 6. Lack of detectable IRF-1, correlates with the loss of silencing effect and virus-inducibility of the C1 oligomer in R66 cells. (**A**) Detection of IRF-1 in nuclear extracts of L929 and R66 cells. Crude nuclear extracts from L929 and R66 cells were subjected to gel shift analysis using end-labeled C1 oligomer as the probe. Lane 1: no extract; lanes 2–4: 4 μg L929 nuclear extract; lanes 5–7: 4 μg R66 nuclear extract; lanes 8–10: 4 μg each of the extracts from L929 and R66 cells; lanes 3, 6, 9: 1000-fold molar excess of cold C1 oligomer; lanes 4, 7, 10: 1000-fold molar excess of cold C5A oligomer. Arrowhead indicates the major complex. (**B**) Loss of silencing and viral induction in R66 cells. Indicated plasmid DNAs were each co-transfected with reference (pRSV*gpt*) gene into L929 and R66 cells to determine transient expression (Materials and methods). Relative CAT activity in mock-induced (filled bar) and NDV-induced (open bar) cells is indicated. The expression level of pSV-55 in each cell line without induction (20 and 85% conversion in L929 and R66 cells, respectively) was considered as 100%. Values are each normalized by comparing the expression level of the reference *gpt* gene.

mRNA was undetectable (<0.1 copy per cell) in the transformants carrying pSV-55C1 and pSV-55C2 whereas other transformants carrying pSV-55C3, pSV-55C4 and pSV-55C5A constitutively expressed the specific mRNA (~ 0.5, 1 and 2 copies per cell, respectively) (Figure 5B). We thus confirmed the silencing effect of the elements (particularly elements C1 and C2) introduced into mouse chromosomes. The results also show that efficiency of the silencing by the various elements is correlated with the previously reported efficiency of their viral-inducibility. The silencing effect is reversible as all the cells expressed mRNA when they were induced by NDV (Figure 5B). The mRNA level after induction increased up to 88 (>880-fold), 78 (>780-fold), 68 (136-fold) and 70 (70-fold) copies per cell with cells containing pSV-55C1, pSV-55C2, pSV-55C3 and pSV-55C4, respectively. Somewhat puzzling is the observation that the accumulated mRNA levels were not found to differ significantly in the induced L929 cells containing those genes. For example, the gene containing C1 and C4 gave

rise to the accumulation of 88 and 58 mRNA copies per cell, respectively, even though one finds a big difference in the inducibility of the two oligomers without the adjoined enhancer (in the stable transformation assay, we found that the C4 oligomer is also inducible but the efficiency was ~50-fold lower when compared to C1 oligomer, unpublished data; see also Fujita *et al.*, 1987). At present, we have no clear explanation; it may be that, in those gene constructs, elements other than IRF-1 binding are involved in determining the mRNA levels in induced cells. Cells bearing pSV-55C5A which gave rise to the highest mRNA expression in uninduced cells also showed a marginal increase in mRNA after induction (four mRNA copies per cell; 2-fold increase).

Loss of silencing and viral induction in cells without detectable IRF-1

The above findings imply the bidirectional property of IRF-1; i.e. involvement of IRF-1 in virus-induced activation of transcription and silencing of the enhancer. If so, cells which lack IRF-1 or contain very low levels of IRF-1 will neither respond to viral induction nor silence the enhancer activity.

On the basis of gel shift assay results, most of the human, monkey and murine cells tested appear to express IRF-1, albeit at different levels (data not shown). However, we found that a monkey cell line, R66, contains very low, if any, IRF-1 in the nucleus as shown by gel shift analysis (Figure 6A). A weak band that migrated faster than IRF-1 protein–DNA complex was detected. The nature of this band is obscure at present. This cell line has been known as an IFN non-producer (Taguchi *et al.*, 1979; Nelson-Ress *et al.*, 1981). The expression of pSV-55, which contains SV40 enhancer juxtaposed to the truncated IFN-β promoter, pSV-55C1 and pSV-55C5A were determined in R66 and L929 cells. In this study, we employed a rapid transient expression system (Fujita *et al.*, 1987). In contrast to L929 cells, CAT expression level of pSV-55C1 and pSV-55C5A in R66 cells is almost equal and their expression levels remain unchanged following induction (Figure 6B). Thus, R66 cells failed to show the silencing of SV40 enhancer and induction by NDV. In both cell lines, expression of pSV-55C5A is lower than that of pSV-55, indicating a distance effect between the SV40 enhancer and IFN-β promoter (in pSV-55C5A, the SV40 enhancer is placed 37 bp further upstream) (Wasylyk *et al.*, 1984).

Discussion

Identification of IRF-1

We identified a nuclear factor, termed IRF-1, that specifically binds to upstream regulatory (virus-inducible) elements of the IFN-β gene. The factor appears to exist in both virus-induced and mock-induced L929 cells. As shown in Figure 1, gel shift assays revealed the appearance of three kinds of factor–DNA complexes and the appearance of two of these complexes is inhibited by DNAs containing the inducible elements. At present, the possibility that two kinds of factors are involved in the formation of those complexes cannot strictly be ruled out. An interesting possibility is that IRF-1 consists of a family of proteins the genes of which are very closely related to each other. As inhibition of complex formation is highly sequence specific to the competitor DNA and the formation of both complexes was barely detectable in R66, then the likely possibilities are that the difference between complex 1 and 2 is a reflection of the different numbers of IRF-1 molecules bound to the probe DNA with repetitive hexanucleotide motifs, or that some of the IRF-1 may be processed or degraded (either in intact cells or during isolation), giving rise to such different complexes. In this regard, when we performed the gel-shift assay by using the synthetic hexamer repeats (depicted in Figure 1C) as the probe, C13 (three repeats) gave rise to only one shifted band, whereas C1 (four repeats) gave rise to two shifted bands (data not shown). This observation may argue for the former possibility. IRF-1 may be similar or equivalent to PRDI-BF detected by Keller and Maniatis (T.Maniatis, personal communication).

Interaction of IRF-1 with the regulatory elements in IFN-β gene expression

IRF-1 appears to recognize the IFN-β gene inducible elements as well as the synthetic hexanucleotide sequences each of which functions as a virus-inducible element. In fact, the IRF-1 binding to the IFN-β gene is sequence specific and it is inhibited by IFN-β upstream sequences and synthetic oligomers functioning as virus-inducible elements and, to a lesser extent, by the VRE of human IFN-α gene (Ryals *et al.*, 1985). The results may indicate that a factor(s) other than IRF-1 is also involved in the IFN-α gene expression. We present experimental evidence that affinity of the genes with various point mutations to IRF-1 as judged by the *in vitro* footprinting patterns is in tight correlation with the inducibility of each mutant gene (Figure 3). These findings strongly argue for the involvement of IRF-1 in the virus-induced transcriptional activation of the IFN-β gene.

The results with the mutant genes (Figure 3) re-emphasize unequivocally the functional importance of the previously identified upstream region and support our previous notion that the repeated hexanucleotide motifs are primarily responsible for induction-specific IFN-β gene transcription (Fujita *et al.*, 1985, 1987). From our footprinting experiments, one could envisage certain co-operative properties of the factor binding to IFN-β gene sequences, as the mutations in block 1, 2, 6 and 7 (i.e. p-125DPcat) were found to dramatically diminish the protection of other unchanged blocks by IRF-1. Our results also show that IRF-1 has a higher affinity to blocks 6 and 7 compared to others. In the experiments reported here, we could not demonstrate specific IRF-1 binding to blocks 1 and 2 which apparently have lower affinity to the factor, even though these blocks seem to play a role in the IRF-1 binding to other blocks (Figure 3B) and the viral-induction of the gene (Figure 3C). In this regard, it may be interesting to try to create up-mutants by converting the blocks to high affinity ones (such as AAGTGA) to IRF-1.

Results of the footprinting analysis may provide a clue to the understanding of the previously described discrepancy reported by many groups on the different sequences required for the IFN-β gene expression. Previously, we presented evidence that the critical 5′ boundary of the IFN-β gene sequence required for maximal induction lies between −117 and −105, and that the inducibility is reduced dramatically by extending the deletion to −93 (Fujita *et al.*, 1985, 1987). A similar conclusion was also reached by Dinter *et al.* (1983). On the other hand, Zinn *et al.* (1985) and Goodbourn *et al.* (1985) concluded that the critical 5′ boundary for induction lies between −79 and −75 (−77 and −73 by their

numbering) in mouse C127 cells transformed by a bovine papilloma virus-derived vector. Only in a transient expression system using the C127 cells, the additional sequence spanning up to −109 appears to be required for maximal induction (Goodbourn *et al.*, 1985). Those results look discrepant *prima facie* but may be worth recapitulating in light of the nature of IRF-1 binding to the regulatory elements reported in this study. The IRF-1 may exist in different levels or in different forms, depending on the state of the cells. Under certain circumstances, the highest affinity blocks (i.e. blocks 6 and 7) for IRF-1 may be sufficient to sustain inducibility, whereas additional blocks are required to insure induction in other circumstances (possibly a co-operative IRF-1 binding to those blocks). From some of the previous data we assume that IRF-1 is partly in active form without further induction in certain cells (for example, see Figure 1A of Goodbourn *et al.*, 1986 and Figure 8 of Fujita *et al.*, 1987), giving rise to constitutive gene expression. Further structural and functional analysis of IRF-1 will be required to clarify this point.

IRF-1 and the silencing effect

Silencing of enhancers by the virus-inducible elements can be observed in both transient (Kuhl *et al.*, 1987; in Fujita *et al.*, 1987) and stable gene transfer systems (this work). In view of the findings that the binding affinity to IRF-1 and the magnitude of silencing activity of hexamer repeats are in good correlation (Figure 5) and that IRF-1 is present in uninduced cells, it is a likely possibility that IRF-1 binding is also involved in the silencing effect. We presume that, in reversing the silencing effect by viral induction, both SV40 enhancer and inducible elements (i.e. enhancer binding factors and active form of IRF-1) co-operate with each other, through yet unknown mechanisms, in the activation of distal gene transcription. The idea is supported by the observation that no silencing and induction occurred in R66 cells (Figure 6).

Possible mechanism of induction and silencing by IRF-1

If the idea put forth above is correct, then how is the induction and silencing brought about by IRF-1? Several possibilities emerge from our observations and previous studies on other genes. Either modification of IRF-1 (model 1) or its association with or dissociation from an additional regulatory protein(s) (model 2) can be postulated as an induction-specific event. In model 1, IRF-1 is present in active and inactive form in induced and uninduced cells, respectively. It is possible that a part of the pre-existing IRF-1 molecules goes through a modification(s) such as phosphorylation as shown in the heat shock factor of yeast (Sorger *et al.*, 1987). Also, it remains to be seen if *de novo* IRF-1 synthesis is required for the efficient induction, in view of the observation that IRF-1 level is increased, albeit modestly, in NDV-induced L929 cells (data not shown). In uninduced cells, the inactive form of IRF-1 may be bound to inducible elements and silence the enhancer function by interfering in factor-mediated interactions between promoter (including TATA box) and upstream enhancer. Such a model has been proposed previously by Kuhl *et al.* (1987). When the cells are induced, the inactive IRF-1 molecules are replaced with the active one, resulting in the activation of the downstream promoter. In model 2, the primary role of IRF-1 is to recognize the inducible elements and an additional factor(s) may be involved in rendering the DNA−protein complex into a transcriptionally active state. Such a model is evoked in the case of yeast GAL4 protein the activity of which is controlled by an additional protein GAL80 (Ma and Ptashne, 1987; Johnston *et al.*, 1987). Whatever the mechanisms, the results presented in Figure 4 may be taken as additional supporting evidence that IRF-1 participates in the induced IFN-β gene expression by forming induction-specific complexes with the regulatory *cis*-elements. However, we cannot strictly rule out the possibility for the presence of distinct factors which recognize the same DNA sequence and each of which plays a role in either induction or silencing, or both.

In view of the fact that possible recognition sequences for IRF-1 are present within other cytokine genes (Fujita *et al.*, 1987; Yasukawa *et al.*, 1987), and non-cytokine (Kuhl *et al.*, 1987; Korber *et al.*, 1988) genes, it is likely that IRF-1 regulates expression of some if not all of those genes either singly or in co-operation with other regulatory factors. Obviously, the factor binding to specific, limited regions of regulatory DNA sequences is a prerequisite, particularly for specific induction of cytokine genes. In this context, the binding and the functional properties of IRF-1 described in this study may be significant for the switching on and off in gene expression.

Materials and methods

Synthetic DNA

Double-stranded DNA oligomers were obtained by annealing the chemically synthesized complementary strands. The sequences of C1, C2, C3, C4, C13 and C12 oligomer DNA were previously described by Fujita *et al.* (1987). The C5A oligomer was obtained by annealing 5′-TC$(GAAA)_6$-GGACTCTAGAG-3′ and 5′-GATCCTCTAGAGTCC$(TTTC)_5$TT-3′. Two complementary strands each 52 nt long were synthesized so as to cover the 42 bp regulatory sequence of IFNα1 gene (−109 to −64, Ryals *et al.*, 1985). The DNA segment contains *Sal*I and *Hin*dIII recognition sites at its upstream and downstream ends, respectively.

Construction of plasmids

The plasmid p-125cat was constructed as p-105cat (Fujita *et al.*, 1987), except the *Bam*HI (−125)−*Taq*I(+19) fragment from pSE-125 (Fujita *et al.*, 1985) was used. Plasmids p-125Dcat, p125Pcat and p-125DPcat each carrying point mutations within the IFN-β regulatory elements were obtained by synthetic oligonucleotide directed mutagenesis on p-125cat essentially as described previously (Hatakeyama *et al.*, 1986). The plasmid pSV-55 was constructed by ligating the following three pieces of DNA: (i) 74 bp *Bam*HI−*Hin*dIII fragment from p-55C1A (Fujita *et al.*, 1987), (ii) 5 kb *Sal*I−*Hin*dIII fragment from pA10cat2 (Rosenthal *et al.*, 1983), whose *Sal*I site was rendered flush by filling in, (iii) 187 bp *Pvu*II−*Bam*HI fragment (encompassing SV40 enhancer, 272−95) from pSV-39I (Fujita *et al.*, 1985). This fragment also contains an *Xho*I site adjacent to the *Bam*HI site. Plasmids pSV-55C1, pSV-55C2, pSV-55C3, pSV-55C4 and pSV-55C5A were constructed by ligating the 74 bp *Bam*HI−*Hin*dIII fragment from p-55C1A (above), the 5 kb *Xho*I−*Hin*dIII fragment from pSV-55 and one of the above described double-stranded oligomers (C1, C2, C3, C4 and C5A).

pRSV*Ecogpt* was constructed by ligating the following fragments: (i) the *Hin*dIII−*Bam*HI fragment from pSV2*Ecogpt* (Mulligan and Berg, 1981) which encompasses *gpt* structural gene, (ii) the large *Hin*dIII−*Bam*HI fragment from pRSV*neo* (Gorman *et al.*, 1983).

DNA transfection, CAT, gpt activity assay and S1 mapping

DNA transfection was performed by calcium phosphate method (Fujita *et al.*, 1985). For transient gene expression analysis, 5×10^6 of L929 cells or 3×10^6 of R66 cells were transfected with 7.5 μg of the test plasmid containing the CAT reporter gene and 2.5 μg of pRSV*gpt* (reference gene). Cells were induced by NDV and harvested as described previously (Fujita *et al.*, 1987). Harvested cells were divided into two groups. One half of the cells was subjected to CAT activity assay (Fujita *et al.*, 1987), the other half was subjected to *gpt* activity assay as described by Shimada (1987).

To obtain stable transformants containing the various CAT constructs, 1×10^6 of L929 cells were transfected with 2 μg of pRSV*neo* (Gorman *et al.*, 1983) and 8 μg of each CAT plasmid. The G418 resistant cells were selected in medium containing 700 μg/ml of G418. Usually 30–60 colonies were obtained in each transfection and they were cultivated as a mixture. This procedure has been used to average out the possible fluctuations observed with individual colonies (Mantei and Weissmann, 1982; Ryals *et al.*, 1985; Fujita *et al.*, 1985) Blot analysis of chromosomal DNA of such a mixture of transformants revealed that ~20 copies per cell of intact CAT gene was integrated.

S1 mapping was performed as described previously, except that the probe was labeled at the 5′ terminus. For the IFN–CAT chimeric gene, a 227 nt long probe encompassing −55 to +172 (numbering IFN-β cap site as +1) was used. RNA copy number was calculated essentially as described previously (Fujita *et al.*, 1987). For the endogenous mouse IFN-β gene, a 104 nt long probe encompassing −15 to +89 was used.

Nuclear extract

All buffers used for the preparation of nuclear extract were supplemented with 0.5 mM PMSF and 10 mM sodium molybdate. The induced extract was made from cells which had been induced for 10 h by Newcastle disease virus (NDV). Nuclei were isolated as described by Higashi (1985). Crude nuclear extract was made as described by Dignam *et al.* (1983). We usually obtained 1 mg protein extract from 5×10^7 cells. For further fractionation, crude extract (25 mg protein) was loaded on to Heparin Sepharose column (2 ml bed), washed extensively with buffer D (Dignam *et al.*, 1983) containing 100 mM KCl. Elution was performed with buffer D containing 200, 300, 400 and 500 mM KCl. Since most of IRF-1 activity was eluted with 200 and 300 mM KCl, mixture of these fractions was used for binding analysis.

DNA affinity column chromatography

Two pieces of synthetic DNA, 5′-$(AAGTGA)_4$-3′ and 5′-$(TCACTT)_4$-3′ were phosphorylated, annealed, ligated and then coupled to CNBr activated Sepharose as described by Kadonaga and Tjian (1986). The affinity resin thus prepared retained 7.5 μg DNA/ml of bed volume. Crude nuclear extract was dialyzed against buffer Z (Kadonaga and Tjian, 1986) and made up to 0.4 mg/ml salmon sperm DNA, 0.1% NP-40, then applied to DNA Sepharose. Elution was done as described by Kadonaga and Tjian (1986).

Preparation of the whole cell extract

L929 cells (1.3×10^8 cells) were harvested by rubber policeman from cell culture dishes, washed once with phosphate-buffered saline (PBS) and collected by centrifugation. The cell pellet (1 ml volume) was frozen at −80°C, then thawed by the addition of 3 ml of lysis buffer (20 mM Hepes, pH 7.9, 0.2 mM EDTA, 0.2 mM EGTA, 0.5 mM spermidine, 0.15 mM spermine, 1 mM DTT, 10% glycerol, 0.5 mM PMSF, 1 μg/ml pepstatin A, 1 μg/ml leupeptin, 500 μM L-1-tosylamide-2-phenylethylchloromethyl ketone, 25 μM *N*-α-*p*-tosyl-L-lysine chloromethyl ketone, 0.5 mM Benzamidine, 10 mM sodium molybdate, 2 mM sodium pyrophosphate, 2 mM sodium orthovanadate). Then, 2 M KCl was added in volume equivalent to one cell pack gradually and gently mixed for 30 min at 4°C. The mixture was centrifuged in a 50Ti rotor at 30 000 r.p.m. for 60 min at 4°C. The supernatant was collected and immediately diluted 5-fold with lysis buffer. The precipitate was removed by centrifugation. The extract in the supernatant contained ~3 mg protein/ml.

Gel shift analysis

The following binding mixture (10 μl) was incubated for 20 min at 25°C: 20 mM Hepes, pH 7.6, 0.5 mM DTT, 0.1 mM EGTA, 1 mM $MgCl_2$, 4% Ficoll, *Escherichia coli* DNA 1 μg, poly dI–dC : poly dI–dC 2 μg, ^{32}P-probe 1–5 fmol, extract 1–5 μg protein, and the indicated amount of unlabeled competitor DNA. The mixture was electrophoresed as described by Singh *et al.* (1986). In this experimental condition, it seems that the IRF-1 is present in excess over the probe DNA, since increasing the probe concentration resulted in an increase of the shifted bands (unpublished observation). This could at least partly explain the fact that relatively high concentrations of unlabeled DNA are required for the competition (Figure 1B and C).

Footprint analysis

The following binding mixture (20 μl) was incubated for 15 min at 0°C: 25 mM Tris–HCl, pH 7.9, 6.25 mM $MgCl_2$, 50 mM KCl, 1 mM EDTA, 0.5 mM DTT, 10% glycerol, 2% polyvinylalcohol, ^{32}P-end-labeled probe 4 fmol, extract 1.5–3.0 μg protein, poly dI–dC:poly dI–dC 0.5 μg, indicated amount of unlabeled competitor DNA. The mixture was then treated with DNase I and analyzed by denaturing gel electrophoresis as described (Lefevre *et al.*, 1987).

Acknowledgements

We thank Drs C.Weissmann and E.Barsoumian, for critical reviews of the manuscript and valuable comments. We also thank Ms M.Sonoda for her excellent assistance. The work is supported in part by a grant-in-aid for Special Project Research, Cancer Bioscience from the Ministry of Education, Science and Culture of Japan.

References

Banerji,J., Rusconi,S. and Schaffner,W. (1981) *Cell*, **27**, 299–308.
Dignam,J., Lebovits,R. and Roeder,R. (1983) *Nucleic Acids Res.*, **11**, 1457–1489.
Dinter,H., Hauser,H., Mayr,U., Lammers,R., Bruns,W., Gross,G. and Collins,J. (1983) In De Maeyer,E. and Schellekens,H. (eds), *Biology of the Interferon System 1983*. Elsevier, Amsterdam, pp. 33–34.
Fujita,T., Ohno,S., Yasumitsu,H. and Taniguchi,T. (1985) *Cell*, **41**, 489–496.
Fujita,T.,Shibuya,H., Hotta,H., Yamanishi,K. and Taniguchi,T. (1987) *Cell*, **49**, 357–367.
Goodbourn,S., Zinn,K. and Maniatis,T. (1985) *Cell*, **41**, 509–520.
Goodbourn,S., Burstein,H. and Maniatis,T. (1986) *Cell*, **45**, 601–610.
Gorman,C., Padmanabhan,R. and Howard,B. (1983) *Science*, **221**, 551–553.
Hatakeyama,M., Minamoto,S. and Taniguchi,T. (1986) *Proc. Natl. Acad. Sci. USA*, **83**, 9650–9654.
Higashi,Y. (1985) *Nucleic Acids Res.*, **13**, 5157–5172.
Johnston,S., Salmeron,J. and Dinchner,S. (1987) *Cell*, **50**, 143–146.
Kadonaga,J. and Tjian,R. (1986) *Proc. Natl. Acad. Sci. USA*, **83**, 5889–5893.
Korber,B., Mermod,N., Hood,L. and Stroynowski,I. (1988) *Science*, **239**, 1302–1306.
Kuhl,D., de la Fuente,J., Chaturvedi,M., Parimoo,S., Ryals,J., Mayer,F. and Weissmann,C. (1987) *Cell*, **50**, 1057–1069.
Lefevre,C., Imagawa,M., Dana,S., Grindlay,J., Bodner,M. and Karin,M. (1987) *EMBO J.*, **6**, 971–981.
Lengyel,P. (1982) *Annu. Rev. Biochem.*, **51**, 251–282.
Ma,J. and Ptashne,M. (1987) *Cell*, **50**, 137–142.
Mantei,N. and Weissmann,C. (1982) *Nature*, **297**, 128–132.
Maruyama,M., Shibuya,H., Harada,H., Hatakeyama,M., Seiki,M., Fujita,T., Inoue,J.-I., Yoshida,M. and Taniguchi,T. (1987) *Cell*, **48**, 345–350.
Maxam,A. and Gilbert,W. (1980) *Methods Enzymol.*, **65**, 499–560.
Mulligan,R.C. and Berg,P. (1981) *Proc. Natl. Acad. Sci. USA*, **78**, 2072–2076.
Nelson-Ress,W., Daniels,D. and Flandermayer,R. (1981) *Arch. Virol.*, **67**, 101–104.
Ohno,S. and Taniguchi,T. (1981) *Proc. Natl. Acad. Sci. USA*, **78**, 5305–5309.
Ohno,S. and Taniguchi,T. (1983) *Nucleic Acids Res.*, **11**, 5403–5412.
Rosenthal,N., Kress,M., Gruss,P. and Khoury,G. (1983) *Science*, **222**, 749–755.
Ryals,J., Dierks,P., Ragg,H. and Weissmann,C. (1985) *Cell*, **41**, 497–507.
Shimada,T. (1987) *Nucleic Acids Res.*, **15**, 4992.
Singh,H., Sen,R., Baltimore,D. and Sharp,P. (1986) *Nature*, **319**, 154–158.
Sorger,P., Leuris,M. and Pelham,H. (1987) *Nature*, **329**, 81–84.
Stewart,W.E.,II (1979) *The Interferon System*. Springer-Verlag, New York.
Taguchi,F., Toba,M. and Tada,A. (1979) *Arch. Virol.*, **60**, 347–351.
Taniguchi,T. (1988) *Annu. Rev. Immunol.*, **6**, 439–464.
Wasylyk,B.,Wasylyk,C. and Chambon,P. (1984) *Nucleic Acids Res.*, **12**, 5589–5608.
Weissmann,C. and Weber,H. (1986) *Prog. Nucleic Acid Res. Mol. Biol.*, **33**, 251–300.
Yasukawa,K., Hirano,T., Watanabe,Y., Muratani,K., Matsuda,T., Nakai,S. and Kishimoto,T. (1987) *EMBO J.*, **6**, 2939–2945.
Zinn,K., Dimaio,D. and Maniatis,T. (1983) *Cell*, **34**, 865–879.

Received on May 6, 1988; revised on June 30, 1988